

circuits.

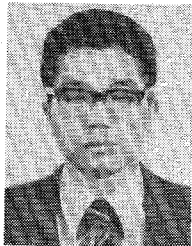
Dr. Ogawa is a member of the Institute of Electronics and Communication Engineering of Japan.

Dr. Yamamoto is a member of the Institute of Electronics and Communication Engineers of Japan.



Kazuyuki Yamamoto (M'76) was born in Kyoto, Japan, on July 13, 1946. He received the B.S., M.S., and Ph.D. degrees in electrical engineering, from the University of Kyoto, Japan, in 1969, 1971, and 1982, respectively.

Since joining the Electrical Communication Laboratory, Nippon Telegraph and Telephone Public Corporation, Tokyo, Japan, in 1971, he has been engaged in the research and development of filters, solid-state circuits, and transmission lines for millimeter-wave systems. He is currently a Staff Engineer of the Radio Transmission Section, Integrated Transmission System Development Division, Yokosuka Electrical Communication Laboratory, NTT.



Nobuaki Imai was born in Kochi, Japan, in 1953. He received the B.S. degree in electrical engineering from Nagoya Institute of Technology, Nagoya, Japan, in 1975, and the M.S. degree from Kyoto University, Kyoto, Japan, in 1977.

Since joining Yokosuka Electrical Communication Laboratories, Japan, in 1977, he had been engaged in the research of millimeter-wave integrated circuits. He is currently engaged in the research and development of VHF band monolithic integrated circuits.

Mr. Imai is a member of the Institute of Electronics and Communication Engineers of Japan.

Analysis and Design of a Single-Resonator GaAs FET Oscillator with Noise Degeneration¹

ZVI GALANI, SENIOR MEMBER, IEEE, MICHAEL J. BIANCHINI, MEMBER, IEEE,
RAYMOND C. WATERMAN, JR., MEMBER, IEEE, ROBERT DIBIASE,
RICHARD W. LATON, MEMBER, IEEE, AND J. BRADFORD COLE MEMBER, IEEE

Abstract—This paper presents an analysis of a low-noise dielectric resonator GaAs FET oscillator in a frequency-locked loop (FLL), which is used for FM noise degeneration. In this circuit, one resonator serves both as the frequency-determining element of the oscillator and as the dispersive element of the discriminator.

The results of the analysis are used to generate design guidelines. These guidelines were followed in an experimental realization of an X-band circuit. The measured FM noise was -120 and -142 dBc/Hz at 10- and 100-kHz offset frequencies, respectively, and corresponded closely to predicted results.

I. INTRODUCTION

THE increased sophistication of missile and ground radar systems has created the need for stable low-noise solid-state microwave sources with associated FM noise levels that are lower than those realizable with conventional crystal or SAW oscillator-based synthesis techniques.

Various source configurations were considered for this application and compared from the standpoint of FM noise, output power (without post-amplification) complexity, performance sensitivity to extreme environmental conditions, and projected cost. The results favored the use of stable bipolar transistor or GaAs FET fundamental oscillators.

Bipolar transistor oscillators exhibit low FM noise and, in conjunction with high Q resonators, are excellent candidates for radar applications at frequencies up to X-band. The superior high-frequency performance of GaAs FET oscillators has made them attractive for use at X-band and above, but their FM noise performance has been demonstrated to be inferior to that of their bipolar transistor counterparts. The FM noise of GaAs FET oscillators may be reduced with high Q resonators and, in this application, the dielectric resonator was deemed most suitable because of its high Q_U (unloaded Q), small size, ruggedness, low cost, and its compatibility with microstrip circuits.

The improvement in the FM noise of a dielectric resonator GaAs FET oscillator, compared to the FM noise of

Manuscript received May 8, 1984.

The authors are with Raytheon Company, Missile Systems Division, Bedford, MA 01730.

¹Patent pending.

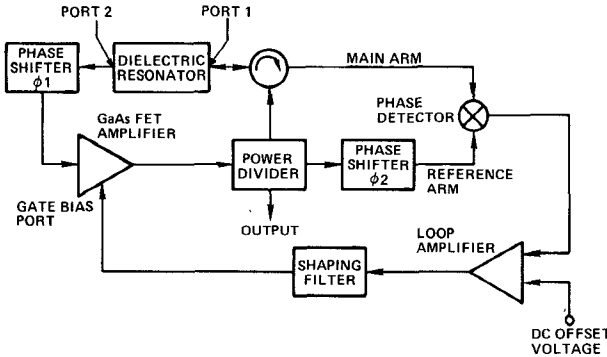


Fig. 1. Block diagram of the GaAs FET oscillator with noise degeneration.

its more conventional microstrip counterpart, is approximated by the ratio of the dielectric resonator Q_L (loaded Q) to the Q_L of the microstrip resonator (for equal resonator insertion losses) [1]. At X-band, the improvement can be as high as 30 dB and is limited by the realizable dielectric resonator Q_U in the oscillator circuit.

The FM noise of an X-band microstrip GaAs FET oscillator has been measured to be typically -65 dBc/Hz at 10-kHz offset from the carrier [2], [3]. Use of a dielectric resonator could reduce this noise to -95 dBc/Hz at the same offset frequency.

Further noise reduction and enhanced frequency stability are achievable with the aid of a frequency-locked loop (FLL), and a novel implementation of such a circuit is shown in Fig. 1 [4]. This paper presents an analysis of that circuit which is used to develop design guidelines.

II. PRINCIPLES OF OPERATION

The unique feature of the circuit shown in Fig. 1 is the dual function served by the dielectric resonator. In the transmission mode, the resonator serves as the frequency determining element of the oscillator feedback circuit, while in the reflection mode it serves as the dispersive element of an interferometer-type of frequency discriminator in the FLL. The use of a common resonator for the two functions eliminates frequency acquisition problems which are characteristic of conventional FLL's.

The oscillator consists of a GaAs FET amplifier with a parallel feedback circuit composed of the transmission mode dielectric resonator (resonant at frequency f_0), phase shifter ϕ_1 , circulator, and power divider. The conditions for commencement of oscillation at f_0 are satisfied if, at that frequency, the small signal gain of the amplifier exceeds the total loss of the feedback circuit (including the effect of power coupled by the power divider) and the phase shift around the loop is an integer multiple of 2π radians.

The FLL consists of the oscillator, frequency discriminator, loop amplifier, and shaping filter. The discriminator is an interferometer [5], [6] with the circulator and resonator in the main arm and phase shifter ϕ_2 in the reference arm. The resonator is connected to the main arm via the circulator and operates in the reflection mode. The power divider couples a portion of the amplifier output power to the reference arm of the discriminator and the oscillator output

port. Most of the output power is routed to the resonator to reduce the effective loss in the feedback circuit. Phase shifter ϕ_2 is adjusted for phase quadrature (at f_0) between the two inputs of the phase detector, resulting in the familiar "S"-shaped relationship between the discriminator output voltage and input frequency. The baseband output of the discriminator is amplified, filtered, and fed back to the gate of the FET through the gate bias port, and a dc voltage is summed into the input of the loop amplifier to provide the FET with the proper gate bias voltage. In this circuit, the gate is the oscillator fine tuning port because the amplifier insertion phase is dependent on the gate voltage. If ϕ_1 were an analog voltage-controlled phase shifter, its control port could have also served as the fine tuning port of the oscillator.

The FLL is designed to degenerate the FM noise of the oscillator. A classical oscillator noise theory [7]–[9] states that this noise is caused by phase uncertainties at the input of the GaAs FET amplifier that are transformed into frequency uncertainties by the phase-frequency relationship of the feedback circuit. These phase uncertainties have two main components: one component is caused by additive white noise in the vicinity of the oscillator frequency, and the second component is caused by phase modulation at baseband frequencies due to random variations of various semiconductor device parameters. The resultant FM noise is detected by the discriminator, the output of which becomes the FLL error signal. The FM noise is degenerated to the noise floor of the loop, typically related to the noise generated by the phase detector diodes.

III. CIRCUIT ANALYSIS AND DESIGN CONSIDERATIONS

The GaAs FET oscillator with noise degeneration (shown in the block diagram of Fig. 1) was developed with the primary goal of realizing the lowest FM noise achievable within the theoretical and practical limits of this implementation. The purpose of this section is to derive the dependence of the oscillator FM noise on certain critical circuit parameters and to develop useful circuit design guidelines.

An analysis of the resonator is presented first, followed by a description of the conditions for oscillation and an analysis of the discriminator. The final part of this section deals with FLL design considerations and is focused on design tradeoffs that have to be performed to achieve optimum FM noise performance.

A. Resonator Analysis

The resonator and its associated coupling structure are modeled by the equivalent circuit of Fig. 2 [10]. This circuit is valid over a narrow frequency range in the vicinity of the resonant frequency f_0 , given by

$$f_0 = \frac{1}{2\pi\sqrt{LC}}. \quad (1)$$

The Q_U of the resonator is expressed as

$$Q_U = R\sqrt{\frac{C}{L}} \quad (2)$$

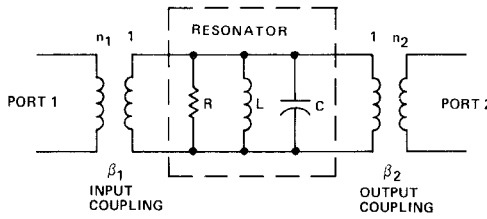


Fig. 2. Equivalent circuit of the resonator and the input and output coupling circuits.

and the external Q 's at ports 1 and 2 of the resonator are defined as

$$Q_{E1} = \frac{Z_{01}}{n_1^2} C \omega_0 \quad (3a)$$

and

$$Q_{E2} = \frac{Z_{02}}{n_2^2} C \omega_0 \quad (3b)$$

respectively, where $\omega_0 = 2\pi f_0$. The corresponding coupling factors β_1 and β_2 are determined from (2) and (3) to be

$$\beta_1 = \frac{Q_U}{Q_{E1}} = \frac{n_1^2 R}{Z_{01}} \quad (4a)$$

and

$$\beta_2 = \frac{Q_U}{Q_{E2}} = \frac{n_2^2 R}{Z_{02}} \quad (4b)$$

and the Q_L of the resonator is defined by the relation

$$\frac{1}{Q_L} = \frac{1}{Q_U} + \frac{1}{Q_{E1}} + \frac{1}{Q_{E2}}. \quad (5)$$

Substituting (4) into (5) and solving for Q_L yields

$$Q_L = \frac{Q_U}{1 + \beta_1 + \beta_2}. \quad (6)$$

The two-port scattering parameters of the equivalent circuit in Fig. 2 were derived for ports 1 and 2 normalized to the (real) impedances Z_{01} and Z_{02} , respectively, and are given by

$$S_{11} = \frac{\beta_1 - \beta_2 - 1 - jQ_U \epsilon}{1 + \beta_1 + \beta_2 + jQ_U \epsilon} \quad (7a)$$

$$S_{21} = \frac{2\sqrt{\beta_1 \beta_2}}{1 + \beta_1 + \beta_2 + jQ_U \epsilon} = S_{12} \quad (7b)$$

and

$$S_{22} = \frac{\beta_2 - \beta_1 - 1 + jQ_U \epsilon}{1 + \beta_1 + \beta_2 + jQ_U \epsilon} \quad (7c)$$

where

$$\epsilon = \frac{f}{f_0} - \frac{f_0}{f}. \quad (8)$$

B. Conditions for Oscillation

The oscillator is composed of the amplifier and the parallel feedback circuit which includes the resonator, circulator, power divider, and phase shifter ϕ_1 . The following conditions must be satisfied for steady-state oscillation at f_0 .

1) The phase shift around the loop consisting of the amplifier and the feedback circuit must be an integer multiple of 2π radians at f_0 . This condition is expressible as

$$\phi_A + \phi_R + \phi_1 + \phi_C = 2\pi k, \quad k = 0, 1, 2, \dots \quad (9)$$

where ϕ_A , ϕ_R , ϕ_1 , and ϕ_C are the respective insertion phases of the amplifier, resonator, phase shifter, and the remaining parts of the feedback circuit, at f_0 . The insertion phase of the resonator is derived from (7b) to be

$$\phi_{21} = \tan^{-1} \frac{-Q_U \epsilon}{1 + \beta_1 + \beta_2}. \quad (10)$$

The insertion phase ϕ_R in (9) is given by

$$\phi_R = \phi_{21}|_{f=f_0} \quad (11)$$

and substitution of (8) and (10) into (11) yields

$$\phi_R = 0^\circ. \quad (12)$$

2) The open-loop small signal gain must exceed unity at f_0 . This condition is expressed as

$$\frac{G_S}{L_R L_C} > 1 \quad (13)$$

where G_S is the small signal gain of the amplifier, L_R is the insertion loss of the resonator, and L_C is the insertion loss of the remaining components of the feedback circuit at f_0 . L_R is given by

$$L_R = \frac{1}{|S_{21}|^2} \Big|_{f=f_0} \quad (14)$$

and substitution of (7b) and (8) into (14) yields

$$L_R = \frac{(1 + \beta_1 + \beta_2)^2}{4\beta_1 \beta_2}. \quad (15a)$$

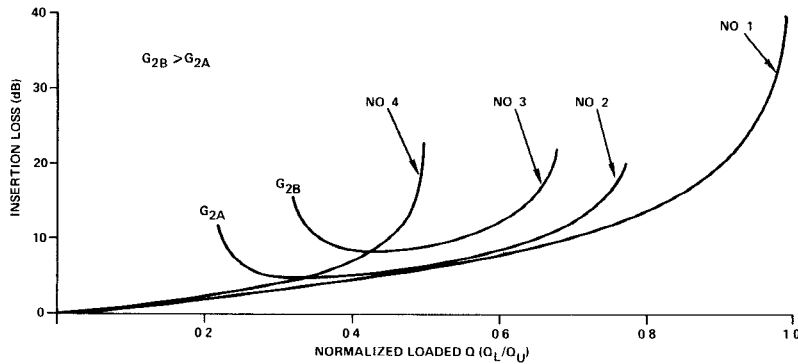
Also, substitution of (4) into (15a) results in

$$L_R = \frac{Q_{E1} Q_{E2}}{4 Q_L^2}. \quad (15b)$$

The extent of the inequality in (13) and the consequent amplifier gain compression in the steady-state oscillatory condition is a topic in itself and is not treated in this paper. Note, however, that excessive amplifier gain compression can adversely affect the oscillator FM noise performance due to an increase in the amplifier noise figure [1], [7], [8] and AM-to-PM conversion.

The oscillator FM noise power spectral density is given by [1]

$$\left(\frac{P_{SSB}}{P_c} \right)_{dBc} = 10 \log \left(\frac{G_L F k T}{P_c} \right) \left(\frac{f_\alpha}{f_m^3 \tau^2} + \frac{1}{f_m^2 \tau^2} + 1 \right) \quad (16)$$

Fig. 3. Resonator insertion loss at f_0 versus normalized loaded Q .

where

P_{SSB} = power in a single FM noise sideband, measured in a 1-Hz bandwidth,

P_c = oscillator total output power (at the amplifier output),

G_L = amplifier gain under steady-state oscillatory conditions = $L_R L_c$,

kT = thermal noise power in a 1-Hz bandwidth = -174 dBm/Hz at room temperature,

F = amplifier noise figure,

τ = resonator transmission phase slope (group delay),

f_α = $1/f$ noise break frequency (in (16) $f_\alpha < 1/\tau$),

f_m = offset or modulation frequency.

This power spectral density is related to the Q_L of the resonator through the variable τ which, with the aid of (6), (8), and (10), is given by

$$\tau = \frac{d\phi_{21}}{df} \Big|_{f=f_0} = \frac{d\phi_{21}}{d\epsilon} \frac{d\epsilon}{df} \Big|_{\epsilon=0} = -\frac{2Q_L}{f_0}. \quad (17)$$

Substitution of (17) into (16) reveals that the oscillator's close-in FM noise exhibits an inverse dependence on Q_L^2 . However, according to (15b), an increase in Q_L results in a higher resonator insertion loss which causes an increase in FM noise and tends to cancel the effect of the higher Q_L . To determine the values of Q_L and L_R that yield the lowest FM noise, expression (15a) is minimized (using the method of Lagrange multipliers) subject to the constraint of a constant Q_L , and yields the condition

$$\beta_1 = \beta_2. \quad (18)$$

Substitution of (5) and (18) into (15b) results in the expression

$$L_{R,\min} = \frac{Q_U^2}{(Q_U - Q_L)^2} \quad (19)$$

which is illustrated graphically (curve #1) in Fig. 3. Substitution of $G_{L,\min}$, given by

$$G_{L,\min} = L_{R,\min} L_c$$

into (16), and differentiation of (16) with respect to Q_L yields the values of Q_L and $L_{R,\min}$ that minimize the FM

noise of the oscillator. They are given by

$$Q_L = \frac{Q_U}{2}$$

and

$$L_{R,\min} = 4 \text{ (6 dB).}$$

These conditions apply to an oscillator without FM noise degeneration. It will be shown that the circuit in Fig. 1 requires a different design methodology to realize the lowest FM noise performance.

C. Discriminator Analysis

From the block diagram of Fig. 1, it is evident that the oscillator performance depends on the transmission-mode characteristics of the resonator, while the discriminator operation is directly dependent on the resonator reflection characteristics at port 1. Using expression (7a), the magnitude and phase of S_{11} , the reflection scattering parameter at port 1, are given by

$$|S_{11}| = \left| \frac{\left[\beta_1^2 - (\beta_2 + 1)^2 - (Q_U \epsilon)^2 \right]^2 + 4\beta_1^2 (Q_U \epsilon)^2}{(1 + \beta_1 + \beta_2)^2 + (Q_U \epsilon)^2} \right|^{1/2} \quad (20)$$

and

$$\phi_{11} = \tan^{-1} \frac{-2\beta_1 Q_U \epsilon}{\beta_1^2 - (\beta_2 + 1)^2 - (Q_U \epsilon)^2} \quad (21)$$

respectively. Evaluating ϕ_{11} at f_0 yields

$$\phi_{110} = \phi_{11}|_{f=f_0} = \begin{cases} 0^\circ, & \beta_1 - \beta_2 - 1 > 0 \\ 180^\circ, & \beta_1 - \beta_2 - 1 < 0. \end{cases} \quad (22)$$

The analysis of the discriminator is based on the diagram of Fig. 4 where it is shown that the amplifier output voltage v_a is given by

$$v_a = V_0 \cos \omega t. \quad (23)$$

Then, since the insertion phases of the two arms of the discriminator can be made identical, except for the contributions of the resonator and phase shifter ϕ_2 , the phase detector input voltages v_1 and v_2 are written by inspection

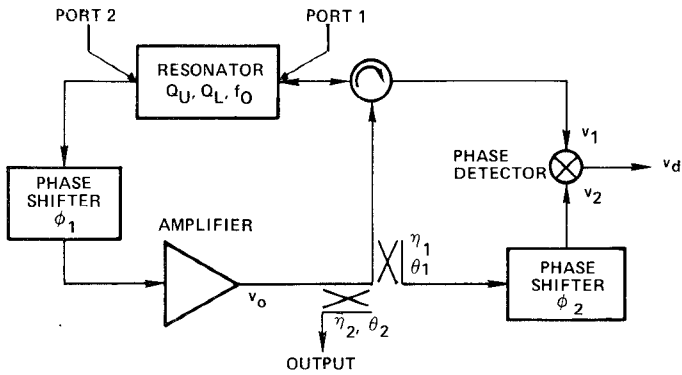


Fig. 4. Block diagram of the oscillator and discriminator circuits.

(assuming loose coupling) as

$$v_1 = |S_{11}|V_0 \cos(\omega t + \phi_{11}) \quad (24a)$$

and

$$v_2 = \eta_1 V_0 \cos(\omega t + \theta_1 + \phi_2). \quad (24b)$$

The discriminator output voltage v_d is given by the product

$$v_d = v_1 v_2. \quad (25)$$

Substitution of (24) into (25) and elimination of the high-frequency terms, because of the low-pass filtering action of the phase detector output port, yields

$$v_d = 0.5 \eta_1 |S_{11}| V_0^2 \cos(\phi_{11} - \theta_1 - \phi_2). \quad (26)$$

If the dependence of v_d on the oscillator frequency is to be characterized by the familiar "S" curve, then v_d must be equal to zero at $f = f_0$. This condition is realized by adjusting the value of ϕ_2 to make the argument of the cosine function in (26) equal to $\pm(\pi/2)$ at f_0 , meaning that

$$\phi_{110} - \theta_1 - \phi_2 = \pm \frac{\pi}{2}. \quad (27)$$

The substitution of (22) into (27) reveals that

$$\theta_1 + \phi_2 = \mp \frac{\pi}{2} \quad (28)$$

and substitution of (28) into (26) yields

$$v_d = \mp 0.5 \eta_1 |S_{11}| V_0^2 \sin \phi_{11} \quad (29)$$

which represents the standard "S"-shaped discriminator output voltage as a function of input frequency.

D. Frequency-Locked Loop Design Considerations

The purpose of the FLL is to degenerate the FM noise of the oscillator to a limit (or floor) determined by the noise sources in the loop and/or the thermal noise floor. Therefore, one of the design goals is to realize an FLL with the lowest possible noise floor.

A simplified block diagram of the FLL is shown in Fig. 5. It includes the dominant noise sources except thermal noise. It will be used to determine the primary contributors to the noise floor of the loop. All the blocks in the diagram are characterized as a function of the offset frequency f_m .

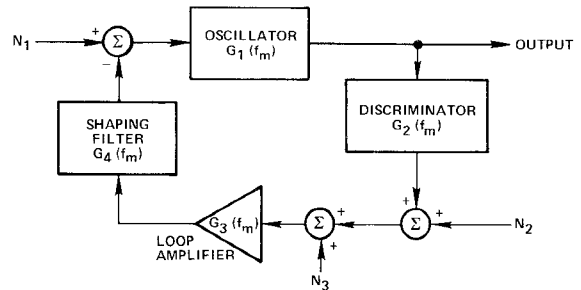


Fig. 5. FLL block diagram, including noise sources.

$G_1(f_m)$ is the oscillator pushing figure defined by the derivative of the output frequency with respect to the FET amplifier dc gate voltage and evaluated at $f = f_0$. $G_2(f_m)$ is the discriminator sensitivity, defined as the derivative of the discriminator output voltage with respect to the input frequency, evaluated at $f = f_0$. $G_3(f_m)$ and $G_4(f_m)$ are the frequency responses of the loop amplifier and of the shaping filter, respectively.

The random noise sources with RMS voltages N_1 , N_2 , and N_3 are statistically independent and are attributed to the nondegenerated oscillator equivalent input noise, the output noise of the discriminator (usually arising from the phase detector diodes), and the equivalent input noise of the loop amplifier, respectively. The FM noise at the output of the FLL, expressed as the RMS frequency deviation $\Delta f(f_m)$, is given by

$$\Delta f(f_m) = \left(\overline{\Delta f_1^2}(f_m) + \overline{\Delta f_2^2}(f_m) + \overline{\Delta f_3^2}(f_m) \right)^{1/2} \quad (30)$$

where Δf_1 , Δf_2 , and Δf_3 are the rms frequency deviations at the FLL output due to N_1 , N_2 , and N_3 , respectively, and are expressed as

$$\Delta f_1 = \frac{N_1 G_1}{1 + G_1 G_2 G_3 G_4} \approx \frac{N_1}{G_2 G_3 G_4} \quad (31)$$

$$\Delta f_2 = \frac{N_2 G_1 G_3 G_4}{1 + G_1 G_2 G_3 G_4} \approx \frac{N_2}{G_2} \quad (32)$$

and

$$\Delta f_3 = \frac{N_3 G_1 G_3 G_4}{1 + G_1 G_2 G_3 G_4} \approx \frac{N_3}{G_2} \quad (33)$$

where the approximations hold for $G_1 G_2 G_3 G_4 \gg 1$.

The relationship

$$\Delta f_2 > \Delta f_1 \quad (34a)$$

will hold as long as the magnitude of the FLL open-loop frequency response exceeds the difference between the oscillator undegenerated noise and Δf_2 . Furthermore, the use of a low-noise loop amplifier also leads to the relationship

$$\Delta f_2 > \Delta f_3. \quad (34b)$$

Thus, in most cases the noise floor of the loop is determined by Δf_2 which, in turn, depends on N_2 and G_2 . With a fixed N_2 , the lowest noise floor is realized with the highest possible discriminator sensitivity. Therefore, an important FLL design consideration is to achieve the maxi-

imum discriminator sensitivity without violating other design constraints.

For $f_m = 0$, the discriminator sensitivity is given by

$$G_2(0) = \frac{\partial v_d}{\partial f} \Big|_{f=f_0} = \frac{\partial v_d}{\partial \epsilon} \cdot \frac{\partial \epsilon}{\partial f} \Big|_{f=f_0}.$$

Performing the differentiation and several lengthy but straightforward algebraic manipulations results in

$$G_2(0) = \mp \frac{\eta_1 V_0^2 S_{11}}{f_0} \frac{\partial \phi_{11}}{\partial \epsilon} \Big|_{f=f_0}$$

which finally reduces to

$$G_2(0) = \pm \frac{2\eta_1 V_0^2}{f_0} \cdot \frac{\beta_1 Q_L^2}{Q_U} \quad (35)$$

where the sign in (35) depends upon the sign in (29).

If V_0 and Q_U are fixed, then the value of $G_2(0)$ depends on β_1 , Q_L , and η_1 . The maximum values of β_1 and Q_L are limited by the insertion loss of the resonator because it determines the thermal noise floor and the gain of the amplifier. The maximum value of η_1 is limited either by the insertion loss of the feedback circuit or the saturation level of the phase-detector diodes.

The optimum FM noise performance of the FLL, therefore, is based on a design tradeoff between the nondegenerated noise of the oscillator and the extent of noise degeneration. The noise of the oscillator depends on its circuit Q_L and, in most cases, is limited by the insertion loss of the resonator and/or amplifier gain. The extent of noise degeneration is limited by loop stability considerations, thermal noise, and the noise floor of the loop.

A design methodology was developed which maximizes normalized discriminator sensitivity for a given resonator insertion loss or, given a required discriminator sensitivity, minimizes the resultant insertion loss of the resonator. Curves relating the resonator insertion loss at f_0 to its Q_L , subject to the constraint of constant normalized discriminator sensitivity, are illustrated in Fig. 3 and are labeled #2 and #3. These curves represent the relation in (35) with $\beta_1 Q_L^2$ held constant and $\eta_1 V_0^2 / f_0$ set equal to unity. Using the method of Lagrange multipliers, it can be shown that the locus of the minimum insertion-loss points on the entire family of curves like #2 and #3 is described by the relation

$$\beta_1 = \beta_2 + 1. \quad (36)$$

This represents the matched condition at f_0 at port 1 of the resonator ($S_{11}|_{f=f_0} = 0$) and is illustrated as curve #4 in Fig. 3. Note that curves #2 and #3 intersect curve #4 at their minimum insertion-loss points. Thus, the intersection of a constant insertion-loss curve (a horizontal line) in Fig. 3 with the highest corresponding discriminator sensitivity curve takes place on curve #4. In fact, substitution of (36) and (6) into (35) yields

$$G_2(0) = \pm \frac{\eta_1 V_0^2 Q_L}{f_0} \quad (37)$$

which indicates that, under the condition stated in (36), $G_2(0)$ is directly proportional to Q_L and is therefore also subject to resonator insertion loss versus Q_L tradeoffs.

To illustrate an example of a design tradeoff, the point on curve #1 in Fig. 3 where $Q_L = Q_U/2$ may be arbitrarily selected as the starting point, because it was determined to be optimum for an oscillator without noise degeneration. A lower FM noise is obtained by selecting a point on curve #4 where the resonator insertion loss is identical to that of the starting point and corresponds to $Q_L = 0.375 Q_U$. At this point, the undegenerated noise of the oscillator is higher by 2.5 dB and, according to (35) and (37) the discriminator sensitivity $G_2(0)$ is higher by 3.52 dB, yielding a commensurately lower noise floor. Thus, an FM noise improvement of 3.52 dB may be realized but it requires an increase of 2.5 dB in the gain of the loop amplifier. The increased discriminator sensitivity and gain of the loop amplifier correspond to a total increase of 6.02 dB in the magnitude of the open-loop frequency response of the FLL.

IV. CIRCUIT DESIGN PROCEDURE

A circuit design procedure is presented herein. It is given in the form of general guidelines and leaves the specifics to the discretion of the designer. The procedure is outlined as follows:

1) The Q_U of the resonator is measured using a coupling structure and a mounting arrangement which are compatible with the oscillator circuit.

2) From the FLL design considerations, it is evident that an increase in G_2 will, to the first order, reduce the FM noise floor of the loop. G_2 depends on the Q_L of the resonator and the power coupled to the reference arm of the discriminator. It is limited by the feedback circuit losses, phase detector diode saturation level, and FLL stability considerations. The insertion loss of the feedback circuit is limited by the gain of the GaAs FET amplifier and the desired level of gain compression. For a given resonator insertion loss, G_2 is maximized if the value of the resonator Q_L is selected on curve #4 in Fig. 3, which also implies a matched condition at f_0 at port 1 of the resonator.

3) The guidelines in step 2) are used to design the oscillator circuit. This circuit is assembled and the following tests are performed:

a) The amplifier output power is measured to determine the power to be coupled to the references arm of the discriminator and to the oscillator output port. Using the specified coupling values, a power divider is designed and incorporated into the circuit.

b) The FM noise of the oscillator is measured with the discriminator ports of the circulator and the power divider terminated with a matched load.

c) The remaining parts of the discriminator circuit are added and the composite frequency response $G_1(f_m)G_2(f_m)$ of the oscillator and discriminator is measured.

4) The minimum detectable frequency deviation at the output of the discriminator is estimated by considering the noise figure of the phase detector diodes, the diode low-frequency resistance, and the discriminator sensitivity.

5) The magnitude of the open-loop frequency response of the FLL is specified to provide degeneration of the oscillator FM noise to a level approaching the noise floor of the loop. This floor is derived from the minimum detectable frequency deviation and can be approached to within 1 dB by specifying the magnitude of the open-loop frequency response of the FLL to exceed by 6 dB the difference between the FM noise of the oscillator and the level of the noise floor. The phase of the open-loop frequency response of the FLL is specified to ensure an adequate stability margin.

6) The composite frequency response of the loop amplifier and shaping filter is determined by subtracting the composite frequency response of the oscillator and discriminator from the desired FLL frequency response, specified in step 5).

7) Using the guidelines in steps 4)–6) an amplifier and a shaping filter are designed, assembled, tested, and incorporated into the circuit. The closed-loop FM noise is measured and compared to predictions. If the measured FM noise is lower than predicted, further improvement in FM noise may be achieved through additional noise degeneration provided by a modification of the magnitude and phase of the FLL frequency response.

V. EXPERIMENTAL RESULTS

The dielectric resonator, mounted in a microstrip test fixture, is shown in Fig. 6. Its resonant frequency was mechanically tuned to 10 GHz and its Q_U was measured to be 4200. The single-stage amplifier, shown in Fig. 7, utilized a Raytheon GaAs FET with 500- μ m gate periphery and had a small signal gain of 10 dB with a 3-dB bandwidth of 300 MHz, centered at 10 GHz.

Assuming that the insertion loss of the resonator is the dominant loss in the feedback circuit, the guidelines in step 2) of the design procedure were followed to maximize G_2 . In order to realize an amplifier gain compression of 1 dB, the insertion loss of the oscillator feedback circuit was limited to 9 dB, which translated to a resonator insertion loss of 7 dB. With this insertion loss, the maximum value of G_2 was obtained (with the aid of curve #4 in Fig. 3) for a Q_L of 1680.

An oscillator circuit was designed and fabricated using the specified value of Q_L verified to be 1624 from the measured transmission characteristic in Fig. 8. The amplifier output power, measured to be +16 dBm, was used to specify a power divider to couple 0 dBm to the reference arm of the discriminator and +6 dBm to the oscillator output port. This power divider was incorporated into the circuit and the FM noise of the oscillator was measured and is shown in Fig. 9.

The assembly of the discriminator was completed and the slope of its "S" curve, shown in Fig. 10, was measured to be 180 mV/MHz.

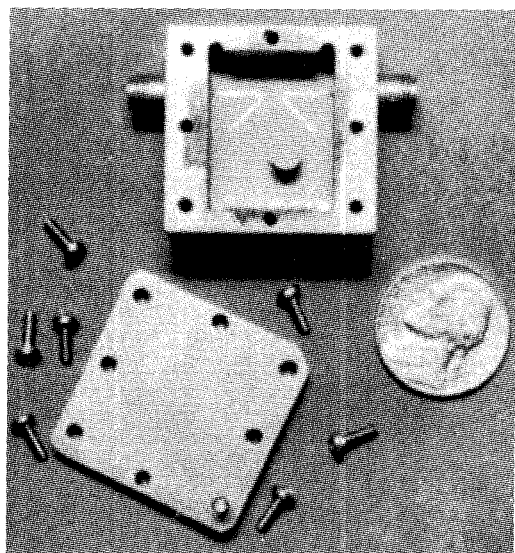


Fig. 6. Dielectric resonator mounted in a microstrip circuit.

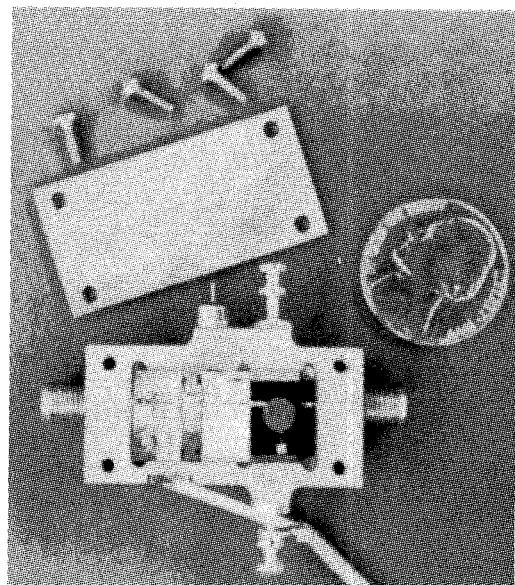


Fig. 7. Single-stage GaAs FET amplifier.

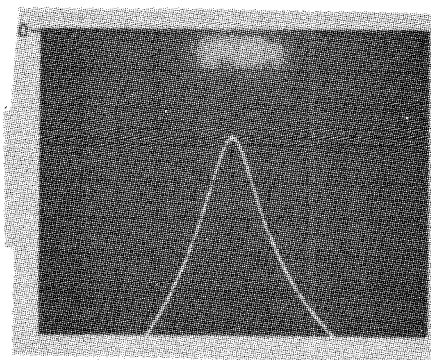


Fig. 8. Dielectric resonator transmission characteristic.

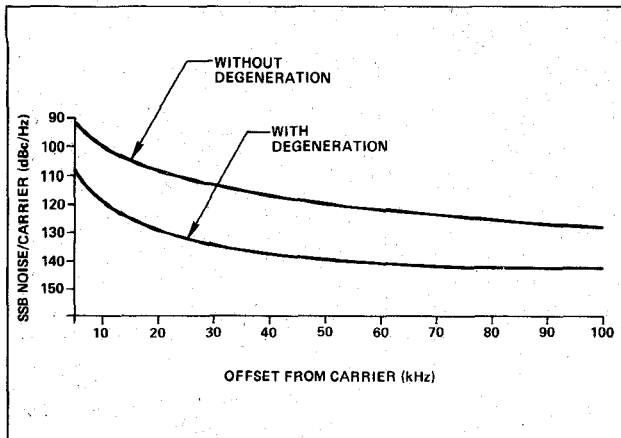


Fig. 9. Measured oscillator FM noise performance.

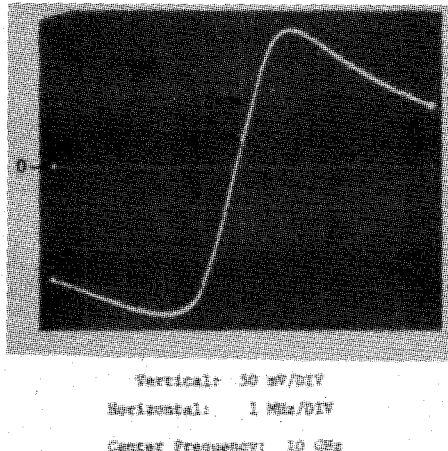


Fig. 10. Discriminator output voltage versus input frequency.

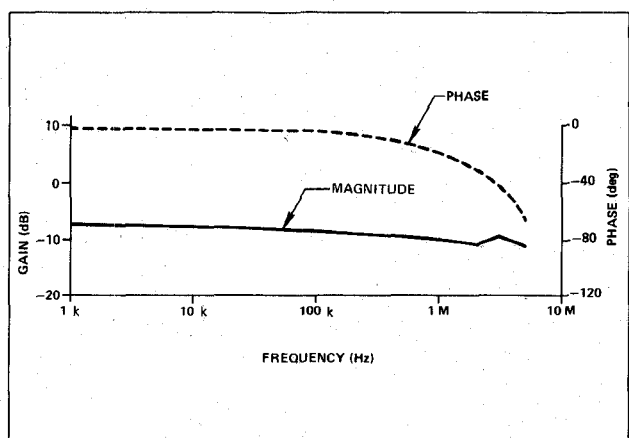


Fig. 11. Oscillator/discriminator composite frequency response.

The measured composite oscillator/discriminator frequency response $G_1(f_m)G_2(f_m)$ is shown in Fig. 11. Also, assuming a phase detector diode noise figure of 10 dB and a low-frequency impedance of 100Ω , the estimated minimum detectable frequency deviation at the output of the discriminator translated to a noise floor of -122 and -142 dBc/Hz at 10- and 100-kHz offset frequencies, respectively.

The measured oscillator FM noise, shown in Fig. 9, corresponds to -100 and -128 dBc/Hz at 10- and 100-kHz offset frequencies, respectively. This noise has a slope of close to 30 dB/decade and hence is described by the first term in (16), which corresponds to the $1/f$ noise of the GaAs FET. To degenerate this noise to a level within 1 dB of the estimated noise floor of the loop, an FLL was required with open-loop frequency response magnitudes of 28 and 20 dB at 10- and 100-kHz offset frequencies, respectively.

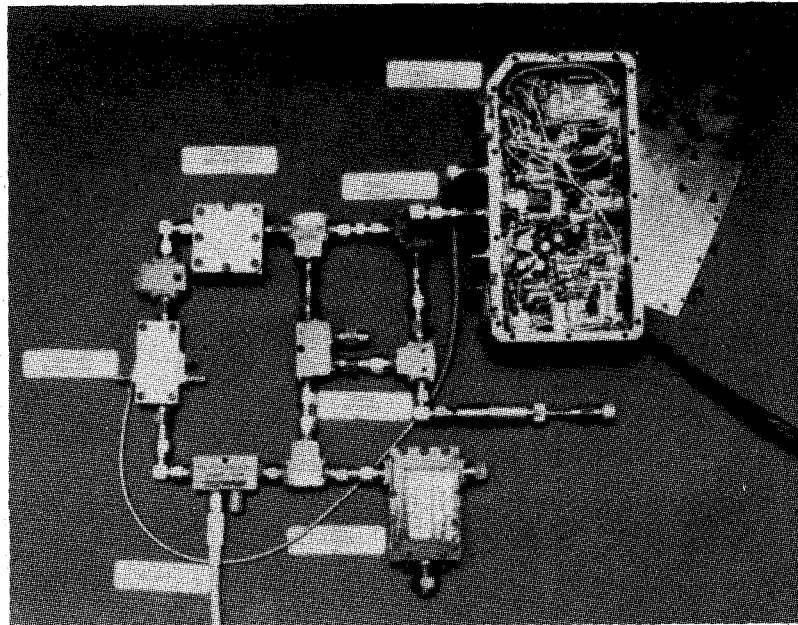


Fig. 12. Dielectric resonator GaAs FET oscillator and FLL circuits.

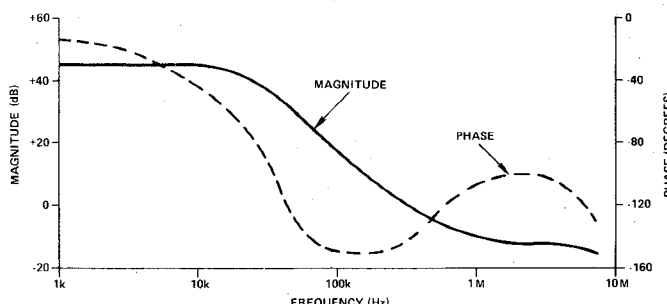


Fig. 13. Measured FLL open-loop frequency response.

The composite frequency response of the loop amplifier/shaping filter was determined using step #6 of the circuit design procedure. The loop amplifier and shaping filter were designed, fabricated, tested, and incorporated into the FLL. A photograph of the complete circuit is shown in Fig. 12, and the measured open-loop frequency response of the FLL is shown in Fig. 13. The measured degenerated FM noise is presented in Fig. 9 and is -120 and -142 dBc/Hz at 10 - and 100 -kHz offset frequencies, respectively. Since the second term in (16) is estimated to be approximately this level, the results imply that most of the GaAs FET-related $1/f$ noise has been degenerated.

VI. SUMMARY AND CONCLUSIONS

A dielectric resonator GaAs FET oscillator with noise degeneration was presented. Critical parts of the circuit were analyzed and a design methodology was developed and presented in the form of design guidelines. These guidelines were used to design a dielectric resonator oscillator and FLL that exhibited the lowest GaAs FET oscillator FM noise published in the literature.

The concept presented in this paper is applicable to electronically tunable oscillators by replacing the dielectric resonator with a tunable resonator such as a varactor-tuned cavity or a YIG filter.

REFERENCES

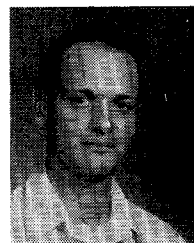
- [1] T. E. Parker, "Current developments in SAW oscillator stability," in *Proc. 31st Ann. Frequency Control Symp.*, pp. 359-364, 1977.
- [2] O. Ishihara, T. Mori, H. Sawano, and M. Nakatani, "A highly stabilized GaAs FET oscillator using a dielectric resonator feedback circuit in 9-14 GHz," *IEEE Trans. Microwave Theory Tech.*, vol. MTT-28, pp. 817-824, Aug. 1980.
- [3] B. T. Debney and J. S. Joshi, "A theory of noise in GaAs FET microwave oscillators and its experimental verification," *IEEE Trans. Electron Devices*, vol. ED-30, pp. 769-776, July 1983.
- [4] M. J. Bianchini, J. B. Cole, R. DiBiase, Z. Galani, R. W. Laton, and R. C. Waterman, Jr., "A single-resonator GaAs FET oscillator with noise degeneration," in *1984 IEEE MTT-S Int. Microwave Symp. Dig.*, pp. 270-273.
- [5] E. H. Katz and H. H. Schreiber, "Design of phase discriminators," *Microwaves*, pp. 26-33, Aug. 1965.
- [6] I. Yuval, "Proper delay line discriminator design avoids common pitfalls," *Microwave Syst. News*, pp. 109-118, Dec. 1982.
- [7] D. B. Leeson, "A simple model of feedback oscillator noise spectrum," *Proc. IEEE*, vol. 54, pp. 329-330, Feb. 1966.
- [8] D. B. Leeson, "Short term stable microwave sources," *Microwave J.*, pp. 59-69, June 1970.
- [9] D. Scherer, "Design principles and test methods of low phase noise RF and microwave sources," in *Hewlett-Packard RF and Microwave Symp.*, pp. 10-15, Oct. 1978.
- [10] J. L. Altman, *Microwave Circuits*. New York: Van Nostrand, 1964, pp. 237-241.



Zvi Galani (S'68-M'72-SM'82) received the B.S.E.E. from the Milwaukee School of Engineering, WI, in 1963 and the M.S. and Ph.D. degrees in electrical engineering from Cornell University, Ithica, NY, in 1969 and 1972, respectively.

From 1963 to 1966, he was employed by the General Electric Company, Communication Products Department in the design of low-noise solid-state microwave sources for multi-channel telecommunication equipment. In 1972, he joined the Bedford Laboratories of Raytheon Missile

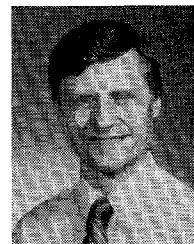
Systems Division, and was involved in the design of microwave sources, GaAs FET amplifiers, and a variety of other microwave circuits. From 1976 to 1982, he was the manager of the Microwave Sources and Devices Section in the Missile Guidance Laboratory and was responsible for directing the development of master oscillators, excitors, and amplifier combining circuits for missile-seeker applications. Since 1982, he has been on the Technical Staff of the Raytheon Bedford Laboratories. He has collaborated on several inventions and has authored papers in the areas of microwave sources, power FET amplifiers, and amplifier combiner circuits.



Michael J. Bianchini (S'76-M'79) was born in Brockton, MA, on August 13, 1955. He received the B.S.E.E. and M.S.E.E. degrees from Southeastern Massachusetts University, North Dartmouth, MA, in 1977 and 1981, respectively.

Since 1979, he has been with the Raytheon Company, Missile Systems Division, Bedford, MA. His primary duties there have been related to the design and development of various microwave oscillators and sources, as well as amplifiers and automated test stations.

Mr. Bianchini is a member of Eta Kappa Nu (Zeta Xi Chapter).

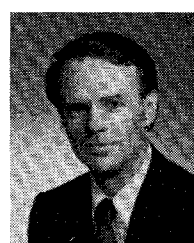


Raymond C. Waterman, Jr. (S'68-M'71) was born in Montague, MA, on February 11, 1946. He received the B.S. degree in electrical engineering from the University of Massachusetts, Amherst, in 1969 and has done graduate studies at Northeastern University, Boston, MA.

Since joining the Raytheon Company, MSD, in 1969, he has worked on microwave devices and subsystems, including receivers and solid-state frequency-locked and phase-locked sources. He has also contributed to the development of

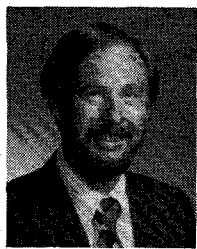
GaAs monolithic microwave integrated circuits and their integration into subsystems. Presently, he is working on stabilized sources at C-band through Ka-band.

Mr. Waterman is a member of Eta Kappa Nu.



Robert DiBiase was born in Somerville, MA, on December 3, 1941. He graduated from Wentworth Institute of Technology, Boston, MA, in 1962 and completed Air Force duty in 1965.

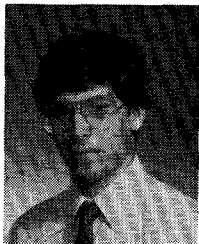
Between 1965 and 1971, he was with Microwave Associates in Burlington, MA. Since 1971, he has been with Raytheon's Missile System Division, and is presently an Engineer in the Microwave and Antenna Department within the Missile Guidance Laboratory.



Richard W. Laton (S'65-M'71) was born in Springfield, IL. He received the B.S. degree from the U.S. Naval Academy and the M.S.E. and Ph.D. degrees in electrical engineering from the University of Michigan, Ann Arbor. The topic of his Ph.D. dissertation, completed in 1972, was "Characteristics of IMPATT Diode Reflection Amplifiers."

He was employed as a staff member at the M.I.T. Lincoln Laboratory, Lexington, MA, from 1972 to 1979, engaged in research and development of solid-state microwave devices and their application to phased-array radars. Since December of 1979, he has been with Raytheon's Missile Systems Division Bedford Laboratories where he has served as section manager for solid-state missile microwave transmitters as well as

for microwave sources and devices. His current position is that of program manager, Ballistic Intercept Missile.



J. Bradford Cole (S'81-M'84) was born in Pittsburgh, PA, in 1960. He received the B.S.E.E. degree from Carnegie-Mellon University, Pittsburgh, PA, in 1982, and the M.S.E.E. degree from the University of Massachusetts, Amherst, in 1984 on a Raytheon Fellowship.

Since 1982, he has been employed by Raytheon Company, Bedford, MA, where he has worked on low-noise oscillator design and multi octave monolithic amplifier design.

RF Spectrum of Thermal Noise and Frequency Stability of a Microwave Cavity-Oscillator

BERNARD VILLENEUVE, STUDENT MEMBER, IEEE, PIERRE TREMBLAY, STUDENT MEMBER, IEEE,
ALAIN MICHAUD, STUDENT MEMBER, IEEE, AND MICHEL TÉTU, SENIOR MEMBER, IEEE

Abstract — The spectral distribution of the thermal noise within a microwave cavity equipped with an external feedback loop has been calculated and measured. An equivalent electrical model is established from which the noise spectral density can be calculated at any port in the system. The effect of the gain and phase of the loop on the spectral distribution is measured with a spectrum analyzer through a heterodyne technique and comparison with theoretical calculations shows good agreement. Also, the modified cavity Q and resonant frequency is measured for various loop parameters. An experimental setup allowing precise measurement of frequency stability and FM noise close to carrier of microwave oscillators is presented and discussed. Preliminary measurements of the short-term frequency stability of the system when operated as a microwave cavity-oscillator show a predominant flicker frequency noise. The measured FM noise close to carrier is related to time-domain measurements of frequency stability and to RF spectrum of the cavity-oscillator.

I. INTRODUCTION

THE QUALITY FACTOR of a microwave cavity can be varied easily over a wide range if it is equipped with an external feedback loop having a variable gain and a variable total phase shift [1]. The Q factor can be reduced or increased, and the system becomes an oscillator when its value reaches infinity. Microwave cavities using such an artificially enhanced Q factor are encountered in

atomic frequency standard technology where small size devices are built using this approach [2]. With this type of standards, it has been observed through frequency stability measurements that the effect of thermal noise within the cavity varies greatly with the parameters of the external loop [3]. We present in this paper a theoretical evaluation of the spectral distribution of this thermal noise for various operating conditions and compare the calculated results to measured data. We give also preliminary results on the study of frequency stability and FM noise for this type of system when operated as a cavity-oscillator.

II. THERMAL NOISE

A. Radio-Electrical Model

The microwave cavity and its feedback loop (or the microwave cavity-oscillator) can be represented schematically through Fig. 1. Power is coupled in and out of the cavity with coupling coefficients β_2 and β_1 , respectively. The external loop consists of a low-noise GaAs FET amplifier, a variable attenuator, a variable phase shifter, and two isolators, one at each end of the loop. The output signal is observed through an AM heterodyne receiver. In this setup, discrete elements are used in order to evaluate separately their contribution to the behavior of the whole system.

Manuscript received May 7, 1984.

The authors are with Laboratoire de recherche sur les oscillateurs et systèmes, Département de génie électrique, Université Laval, Québec, G1K 7P4, Canada.